ROYAL SOCIETY OF CHEMISTRY

Check for updates

Evaluation of airborne particulates and associated metals originating from steel slag applied to rural unpaved roads†

James Kacer, [ID] *[a] Ralph Altmaier,[a] Drew Latta,[b] Patrick T. O'Shaughnessy[a] and David M. Cwiertny [ID] [bc]

Various metals have toxic effects by the inhalation route, and electric arc furnace (EAF) steel slag is known to contain metals with a potential for toxicity to humans. In some states, EAF slag is applied to unpaved (gravel) roads as a low-cost supplement to limestone and other crushed stone, where it may be a public health concern for the local population. This study compared the mass of selected metals in the PM_{10} size fraction of fugitive dust from roads where slag was applied to metals in fugitive dust where slag was not applied. Manganese, designated by the EPA as a hazardous air pollutant (HAP) and one of the primary metals of concern in the slag, was 1.3 times more concentrated in the PM_{10} fraction from the slag-covered roads as compared to the PM_{10} fraction from the non-slag-covered roads, but that increase was not significant ($p = 0.26$). Other metals detected in the airborne dust from both slag-covered and non-slag-covered roads that are also designated as HAPs are antimony, arsenic, chromium, cobalt, lead, nickel, and selenium. In addition, hourly sampling of PM_{10} and metals in the PM_{10} fraction was conducted at one of the sample locations where slag had been applied to the road. Manganese mass in the PM_{10} was positively correlated (Spearman $r = 0.86$) with the particulate mass in the PM_{10}. Wind direction and the interaction of traffic and wind direction were found to be statistically significant factors affecting manganese concentrations in the fugitive emissions from the road to which EAF slag had been applied. This research demonstrated that application of steel slag can result in elevated levels of manganese in the airborne dust generated by vehicular traffic on the unpaved roadway.

Environmental significance

Unpaved roads are a significant source of ambient particulate matter (PM) in rural areas and, therefore constitute a potential health hazard. To address this concern, we assessed airborne concentrations of PM and airborne metals near roads to which electric arc furnace slag had been applied as a supplement to crushed stone. We also evaluated environmental factors, such as wind direction, wind velocity, and traffic volume on the resulting concentration of PM10. This novel research is the first to fully evaluate slag-covered gravel roads as sources of PM and airborne metals. An innovative use of an ambient continuous metal monitor, which analyzed metal concentrations in PM10 on an hourly basis, allowed comparisons to hourly measurements of PM10 and traffic levels. Study results determined that airborne manganese was elevated despite PM10 concentrations being similar between slag-covered and typical gravel roads, which indicates an enrichment of metals in slag-induced PM.

Introduction

A number of metals are known toxicants by the inhalation route,[1,2] with some specifically addressed as hazardous air pollutants (HAPs) in the United States (US) Clean Air Act.[3]

[a]*Department of Occupational and Environmental Health, College of Public Health, University of Iowa, Iowa City, 52242, Iowa, USA. E-mail: james-kacer@uiowa.edu*

[b]*Department of Civil and Environmental Engineering, College of Engineering, University of Iowa, Iowa City, 52242, Iowa, USA*

[c]*Center for Health Effects of Environmental Contamination, University of Iowa, W195 Chemistry Building, Iowa City, 52242, Iowa, USA*

† Electronic supplementary information (ESI) available. See DOI: https://doi.org/10.1039/d2ea00040g

Airborne metals can be emitted from natural sources (*e.g.*, soil) or other sources such as motor vehicles and various industries. One such industrial source that may result in the emission of airborne metals is slag from steel processing, including both blast furnaces and electric arc furnaces (EAF). Slag is produced as a by-product when impurities are removed from the molten steel, having a dark gray to black coloration due to the presence of iron oxides.[4] EAFs use direct application of an electric arc to melt charged steel and is used in the secondary steel-making process (scrap steel is the primary raw material in secondary steelmaking, as opposed to the iron ore and raw pig iron used in primary steelmaking).[5] Slag from both types of furnaces has been sold for use as asphalt aggregate, septic fields, road base,

238 | *Environ. Sci.: Atmos.*, 2023, **3**, 238–246

© 2023 The Author(s). Published by the Royal Society of Chemistry

and embankment fill, among many other uses.[6,7] An estimated 16.3 million metric tons of iron and steel slag were generated in 2019, the most recent year for which data are available, with 52.4% of the 8 million metric tons of blast furnace slag and 44.4% of the 8.3 million metric tons of EAF slag being used for road bases and surfaces (concrete and asphalt aggregate).[8]

Steel slag can contain manganese, iron, silicon, and a variety of other metals,[9,10] including metals that have been designated by the EPA as hazardous air pollutants: antimony, arsenic, cadmium, chromium, cobalt, lead, mercury, nickel, and selenium, in addition to manganese.[3] The chemical composition of the slag can be highly variable based on the composition of the feed material of the secondary steelmaking process, the type of steel made, and the furnace operating conditions.[9] EAF slag has been found to have similar or better physical and mechanical characteristics than crushed stone.[11]

The US Department of Transportation states that slag is used on unpaved roads in some regions, but provides few details about where it is used and the quantities used.[12] For example, slag can be used on gravel roads in Idaho, but no information about the amount used or the locations where it has been applied was found.[13] In Iowa, steel slag was exempted by the state as a designated solid waste,[10] which allows the use of EAF slag to supplement the gravel and crushed rock applied to unpaved roads.

After an extensive literature review, only a few studies were found that addressed rural unpaved roads;[14–20] the focus of most of the identified road dust emission research was on urban roads.[21–35] No peer-reviewed research was identified for either rural or urban unpaved roads that evaluated steel slag as a source of fugitive emissions. Therefore, research on this inhalation exposure scenario is needed.

The primary aims of this study were to compare particulate matter (PM_{10} and $PM_{2.5}$) concentrations and airborne metals concentrations in the vicinity of roads to which EAF slag had been applied relative to near roads to which the slag had not been applied. A secondary aim was to evaluate several potential factors affecting the metal content in the airborne particulates, such as traffic, relative humidity, wind direction, and wind velocity. To achieve these aims, we designed a field sampling program in rural Muscatine and Scott Counties in Iowa for collection of 24-hour PM_{10} and $PM_{2.5}$ samples at a background site and several sites alongside slag-covered roads; collection of meteorological and traffic data; collection of hourly PM_{10} data; and collection of metals data from hourly PM_{10} samples. A general linear model was used to assess the meteorological and hourly data to identify significant factors in the determination of ambient particulate concentrations and metal concentrations associated with those particulates.

A specific priority in this study was to evaluate manganese content in PM given its importance as a potential ingestion and inhalation hazard (designated by EPA as a hazardous air pollutant [HAP]). Manganese concentration is anticipated to be elevated in the slag because manganese is necessary for converting iron to steel with the steel industry consuming over 90% of manganese production, both in the U.S. and world-wide.[36] In fact, a preliminary health analysis conducted by the Iowa Department of Public Health suggested an ingestion risk, particularly for young children, based upon available, albeit limited, characterization of the slag applied to the roadways investigated in this study.[37–39] Characterization of manganese in PM is a necessary step in determining whether the slag also presents inhalation risks to surrounding communities.

Methods

Study design

A total of 3 sample sites were chosen for assessment during this study (Table S1 in the ESI†). They were located along unpaved roads surrounded by crop land, with two sites (sites A and B) located in Muscatine County, Iowa. Muscatine County is one of the Iowa counties that has applied EAF slag to its unpaved roads and has applied it to approximately 350 miles of its roads, with the greatest amount being applied during 2016 and 2017.[38] Site B was selected because slag had been applied to the road and could therefore be compared to site A. A background site, located in Scott County and 3.2 km north of the boundary with Muscatine County, was selected because no slag had been applied to the unpaved roads in Scott County. To provide consistency when comparing PM and metal measurements between the sites that may be affected by atmospheric conditions, all sample sites were selected because they were on the north side of an unpaved road that was oriented approximately east-west. Winds were expected to be generally from the west or southwest during the sampling period, which would carry PM disturbed by road traffic to the sampler intakes. Site A was selected because the road alongside where it is located had one of the heaviest apparent slag applications. Tables S2A and S2B in the ESI† list the analytical results for road dust sample locations where PM samples were collected and for sites where PM samples were not collected, respectively.

Field work was conducted from late July until mid-September 2020, a time of year in which rainfall was expected to be low and the meteorological conditions were conducive to fugitive dust generation from the unpaved roads. Because of the proximity of the sites to one another, meteorological conditions recorded at site A (described below) were assumed to be the same for the other sample sites for purposes of comparing PM levels.

Air samples were collected from the background site and from site A from July 30, 2020 through August 9, 2020 and from August 14, 2020 through August 25, 2020. Electrical power to the sample trailer was not available from August 10th through August 13th due to widespread damage from a wind storm, so samples were not collected from the background site or site A during this time. To compare PM_{10}, $PM_{2.5}$, and metals between sites, Graseby Andersen Model 241 dichotomous samplers were placed at the background and slag sites to collect coarse and fine fractions of ambient particulates on filters for gravimetric PM and metals analyses. Two dichotomous samplers were used for the project, with one sampler remaining at site A for the duration of the project, while the other was placed at the background site and the other slag site for varying lengths of time. The intakes were approximately 4 m above ground level,

© 2023 The Author(s). Published by the Royal Society of Chemistry

Environ. Sci.: Atmos., 2023, **3**, 238–246 | **239**

within the 2–15 m EPA guideline.[40] The intake heights were dictated by the sample trailer dimensions. The flow rate for the coarse samples was approximately 1.67 liters per minute (lpm), while the flow rate for the fine samples was approximately 15.0 lpm. Each sample represented an approximately 24-hour period. Before placement in the dichotomous samplers, PTFE 37 mm filters (No. 225-1709, SKC Inc., Eighty-Four, PA) were placed in a humidity- and temperature-controlled room for a minimum of 24 hours before weighing with a six-decimal-place balance (repeatability: 0.0008 mg) (MT5, Mettler-Toledo, Columbus, OH). After retrieving the filters from the dichotomous samplers, they were placed in the same room for a minimum of 24 hours before weighing with the same balance. Laboratory blanks (in triplicate) were also weighed in order to adjust the mass results of the sample filters. Field blanks were also weighed before and after transport to the sampling site after being placed in the balance room for a minimum of 24 hours before weighing. Dichotomous sampler flow measurements taken with a tetraCal® Air Flow Calibrator (Mesa Laboratories, Inc., Lakewood, CO) were recorded manually at the beginning and end of each sampling period and averaged for calculation of total sample volumes. Sampler flows were calibrated each day before the new sampling cycle was initiated. Flow rates for the other instruments were checked periodically with the same calibrator.

Filter analysis for metals

Filter samples of PM from each site were selected for analysis of metals by inductively-coupled plasma (ICP) using equipment and procedures as detailed in the supplement. Sample site A ($n = 11$) and background site ($n = 11$) results were compared for samples collected on the same days. Results from site B ($n = 8$) were compared to site A results collected on the same days. No background site sampling was conducted while sampling at site B because of the limited availability of sampling devices.

Road dust analysis

Muscatine County applied crushed limestone meeting Iowa Department of Transportation specifications for Class A road rock,[41] which specifies a range of 6–16% fines, which are particles that pass the #200 sieve (75 μm mesh size). Crushed limestone supplied to Muscatine County was generally close to the 16% maximum limit for fines (pre-application), while the slag (pre-application) generally had fines close to the minimum amount of 6% (Table S3†).[42] Slag was applied to the roads at the same loading rate as the crushed limestone, and sometimes at a lower rate, according to the County Engineer. Slag was applied separately from the crushed limestone. Given the difference in percentage of fines between the two materials, more PM was expected to be generated from limestone applied roads relative to slag applied roads. The crushed limestone may also produce more fines after application to the roads as slag has been reported to be more resistant to abrasion than crushed limestone.[43] Slag was applied to Muscatine County roads until mid-2018.[38]

To characterize the undisturbed road dust, samples were collected from the road surface at two locations in Scott County, where slag had not been applied to the unpaved roads, and eight locations in Muscatine County, where slag had been applied to the unpaved roads. Some samples had been collected by a community group prior to the selection of the air sampling sites. After the three air sampling sites were selected, surface samples were collected from the roads adjacent to these locations. The samples were sieved using a #200 sieve (openings of 75 μm). The samples were then digested and analyzed for metals following EPA methodologies: 6010B,[44] 6020A,[45] and 7471A.[46]

To determine the mineralogical characteristics of the road rock, semi-quantitative powder X-ray diffraction (pXRD) analysis of the sieved, bulk road samples was conducted. Quantitative phase analysis with Rietveld refinement was done with the software program MAUD.[47] Calcite, dolomite, and quartz were fit as constituent phases. Several other electric arc furnace slag constituent minerals[48] were included in analysis, but always refined to <2% and did not meaningfully improve the fit statistics. These include magnetite (Fe_3O_4), wustite (FeO), graphite (C), alpha-iron (Fe), merwinite ($Ca_3MgSi_2O_8$), larnite (β-Ca_2SiO_4), srebrodolskite/brownmillerite ($Ca_2(Al,Fe)O_5$), akermanite ($Ca_2MgSi_2O_7$), gehlenite ($Ca_2Al_2SiO_7$), olivine (($Mg,Fe)_2SiO_4$), monticellite ($CaMgSiO_4$) and portlandite ($Ca(OH)_2$).

Field instrumentation

Real-time monitoring of the particulate concentrations in the ambient air was conducted using a beta attenuation monitor (BAM 1020 Continuous Particulate Monitor, Met One Instruments, Inc., Grants Pass, OR) placed in the sample trailer at site A to determine fluctuations in PM_{10} concentrations and mass during the sampling period. The BAM is an EPA reference method[49] for PM_{10} that collected and stored PM_{10} concentrations every hour. An ambient continuous metals monitor (ACMM, Xact 625i, Cooper Environmental, Tigard, OR) was placed alongside the other sampling devices in the trailer at the high-application site (site A). This instrument can simultaneously measure up to 67 elements per hour, with 44 elements measured in the standard configuration, including all of the metals of interest for this project. The air samples are collected on a reel-to-reel filter tape which passes through an X-ray detector as the tape moves from one reel to the other. The inlet is particle size-selective; the PM_{10} inlet was used for this project in order to allow comparability with the sample results from the BAM. This instrument was not capable of simultaneously analyzing both the PM_{10} and $PM_{2.5}$ fractions of the ambient air. As a mechanically-generated particle, road dust is expected to consist primarily of coarse particles,[50] so both devices were set to sample PM_{10} instead of $PM_{2.5}$. The intake flow rate for the ACMM was approximately 16.7 lpm. Meteorological data was collected at site A during each sampling episode with a Davis Vantage Vue meteorological station (Davis Instruments, Hayward, California) to determine wind direction and velocity, temperature, and relative humidity. As part of the exposure assessment process, meteorological data was

240 | Environ. Sci.: Atmos., 2023, 3, 238–246

© 2023 The Author(s). Published by the Royal Society of Chemistry

compared to PM data for each sample collection date to allow for prediction of exposures to PM and metals under varying meteorological conditions.

The gravel road near site A was oriented NNW to ESE (120°) based on the Muscatine County Assessor's website.[51] Wind directions from 120° through 300° (from SE to WNW) were judged to be from the road toward the sample trailer, while wind directions from 300° through 120° (from NW to ESE) were judged to be from the sample trailer toward the road. Traffic levels at each site during the sampling periods were measured using a trail camera (Apeman H45, Shenzhen, China). The camera detects motion, which triggers the shutter to take a photograph. The camera date- and time-stamped the photographs, allowing them to be grouped by date and hour for comparison with data from the other instruments.

Data analysis

Hourly data from site A was analyzed using a general linear model (GLM) to determine the significance of certain factors affecting metals concentrations in the PM, with the significance level set at 0.05. The factors of interest included hourly averages of meteorological conditions (wind direction, wind velocity, temperature, relative humidity) and hourly traffic counts. The model was run in R, version R 4.0.4.[52] The dependent variable was the natural logarithm of the metal (*e.g.*, manganese) concentration as measured by the ACMM (continuous), while the independent variables were traffic level (ordinal), wind speed (continuous), wind direction (continuous), and relative humidity (continuous). After conducting a distribution analysis, the metal concentrations were transformed to their natural logarithms. Significance was tested relative to $\alpha = 0.05$. Because of the low number of samples analyzed for metals by ICP, these results were not subjected to statistical analysis and only qualitative assessments were performed (refer to the ESI† for details).

Results and discussion

Analyses of bulk road surface materials

Analysis of the sieved samples from the background road and EAF-slag amended roads in Scott and Muscatine Counties by pXRD revealed that the primary mineral constituents of the fine materials were calcite ($CaCO_3$, the primary component of limestone), dolomite ($CaMg(CO_3)_2$), and quartz (SiO_2) (Table S4†). The Scott County (background) samples were predominantly dolomite, whereas all Muscatine County samples were

mixtures of calcite and dolomite, likely reflecting varying quarry sources for the original road rock. In all cases, no minerals previously found to be associated with EAF slag[48] were observed in the measurements. The lack of slag-related minerals suggests that either slag-related minerals were below the detection limits of the XRD (detection limits near 2–5%), lack crystalline structure (*i.e.*, are amorphous), or that the slag-related minerals were altered to other secondary minerals (such as calcite) upon exposure to environmental conditions. An analysis of the data shown in Tables S2A and S2B† was conducted in which the two non-slag sites were averaged together and all slag sites were averaged by metal. Fig. S1† shows that the metals concentrations at the background sites were consistently lower than at the slag sites.

Site A PM and PM metals

Ambient PM_{10} concentrations were measured alongside an unpaved (gravel) road to which EAF slag had not been applied (the background site) and were also measured alongside several similar roads to which the slag had been applied. Average coarse PM concentrations were 67.3 µg m^{-3} for the background site (average 3.2 vehicles per hour) and 121.5 µg m^{-3} for samples collected from slag site A (average 7.4 vehicles per hour) during the same period (Table 1). For reference, EPA's National Ambient Air Quality Standard (NAAQS, primary and secondary) for PM_{10} is 150 µg m^{-3} for a 24 hours period, not to be exceeded more than once per year, averaged over three years.[53] However, the average background coarse PM concentration was not statistically different from the average site A coarse PM concentration when normalized by the respective average per hour traffic volume ($p = 0.27$), demonstrating that there was little, if any, difference in PM emissions between a road to which slag had been applied and one that had not had slag applied.

The mass of manganese on the dichot sample filter from each of the two sites, measured by ICP-MS, was compared to the mass of total particulate matter on the same filter in order to provide a basis of comparison between the two sites. Fractions of HAP metals in the coarse (2.5–10 µm) fraction of the PM were calculated (Table 2). The ratio of HAP metals mass to total PM mass (µg manganese/mg PM) was first calculated for the background site. The ratio was then compared to the ratio for site A, resulting in a ratio of a ratio. Average coarse PM manganese concentrations were 1279 ng Mn/mg PM for the background site and 1662 ng Mn/mg PM for samples collected from slag site A during the same period. A comparison of the manganese

Table 1 Comparison of mean (std. dev.) PM_{10} concentrations between the background site and site A during the same 23 days period

	Background			Site A		
	PM_{10} (µg m^{-3})	Traffic counts (vehicles per hour)	PM_{10}/traffic count	PM_{10} (µg m^{-3})	Traffic counts (vehicles per hour)	PM_{10}/traffic count
Average	67.3 (51.3)	3.2 (3.7)	20.8	121.5 (68.8)	7.4 (6.5)	16.4
n	23 days	250 hours		23 days	386 hours	

© 2023 The Author(s). Published by the Royal Society of Chemistry

Environ. Sci.: Atmos., 2023, **3**, 238–246 | **241**

Table 2 Mean (std. dev.) fractions of HAP metal coarse mass (ng) analyzed using ICP-MS to PM coarse mass (mg) at the background (BG) site and site A ($n = 11$ each), and ratios of site A mean fraction to BG mean fraction

	BG ng mg^{-1} ($n = 11$)	Site A ng mg^{-1} ($n = 11$)	t-test p value	LOD ng/filter	Site A/BG
Mn	1279 (1013)	1662 (336)	0.26	6.8	1.30
Cr	412 (711)	184 (61)	0.32	6.6	0.45
Ni	37 (61)	12 (14)	0.21	8.8	0.32
Pb	25 (51)	8.3 (7.0)	0.31	3.9	0.33
Co	9.7 (11)	4.9 (1.1)	0.19	0.94	0.51
As	4.1 (2.0)	2.0 (1.24)	0.012	10	0.49
Sb^a	2.7 (4.0)	1.31 (1.01)	0.28	2.0	0.48
Cd^b	—	—		—	—

^{a} One large outlier excluded. ^{b} No Cd was detected in the majority of the samples. The remaining HAP metals (beryllium, mercury, and selenium) were not analyzed.

fraction in the background site PM to the manganese fraction in the site A PM indicates that the proportion of manganese in the coarse fraction was 1.30 times higher at site A than at the background site (Table 2), but this was not a significant increase ($p = 0.26$). All other HAP metals were higher in the background samples, but the differences from site A were not statistically significant except for arsenic ($p = 0.006$). Similar research could not be identified for comparison or corroboration of these findings. This result conflicts with the results shown in Fig. S1† for road dust metals content. This may be a result of a different metals concentration in the PM that is less than 10 μm as compared to the metals concentration for the larger particles (up to 75 μm) in the sieved samples.

Table S5† provides a comparison between metals concentrations detected by the ACMM relative to concentrations detected by ICP-MS from filter samples at site A. The ICP-MS results were obtained from twelve 24-hour coarse and fine filter dichotomous sampler results, while the ACMM metals averages represent 709 hourly samples collected over several months. During that time, there were twelve days when both ACMM and ICP-MS results were available for manganese at site A. The hourly ACMM measurements corresponding to the 24 h time period in which a filter was sampled were averaged and compared using a paired t-test with the corresponding filter

measurements. For those 12 days, the ACMM results were consistently lower for all days and significantly different than the values measured by ICP-MS ($p < 0.001$) (Table S6†).

Hourly averages for ACMM metals concentrations and BAM PM$_{10}$ concentrations were calculated for a typical three-day period at site A (Table S7†), the same period represented in Fig. 1. The standard deviations are relatively large, presumably because of the large variations in both metal and particulate concentrations over a 24 hours period. As expected, the manganese concentrations were highly correlated with the coincidental PM$_{10}$ concentrations (Spearman $r = 0.86$) over the entire sampling period. The lowest PM and manganese concentrations occurred in the early morning when traffic levels were very low. Chromium and nickel concentrations were also highly correlated with particulate concentrations, while arsenic and selenium were not (Table S8†).

The median concentrations of all HAP metals measured by the ACMM over the entire sampling period were calculated, along with limits of detection and EPA reference concentrations, as available (Table S9†). The relative abundances of metals in the PM$_{10}$ fraction of the PM from site A as measured by the ACMM and averaged over the entire sampling period were also calculated (Fig. S2†). Calcium was excluded from this figure since it represented approximately 67% of the total mass of metals in the PM, presumably because of the crushed limestone and dolomite applied to the road surface.
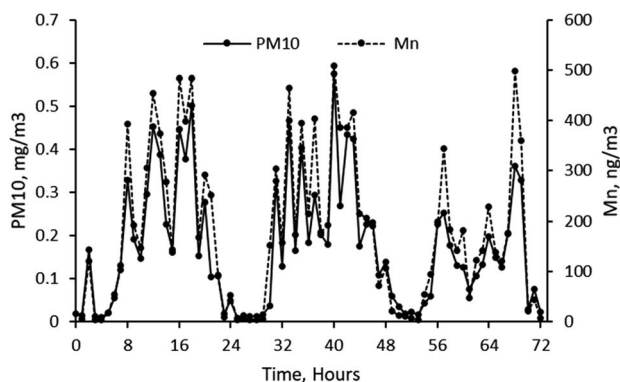

Fig. 1 Hourly PM$_{10}$ and manganese concentrations at site A, showing the cyclical nature of the PM$_{10}$ and manganese data over a three-day period, midnight of August 22 through midnight of August 24, 2020.

PM and manganese comparison between sites

To calculate the fractions of manganese in the coarse fractions of the PM, the ratios of manganese mass to total PM mass (μg manganese/mg PM) were first calculated for each site. The ratio for site B was then compared to the ratio for site A (Table S10†) to evaluate variations in manganese concentrations between these sites. There were non-significant ($p = 0.62$) differences in Mn concentrations between the two sites, with the site B Mn concentrations generally higher than those for site A. The marginal differences between the sites were likely due to different rates of slag application and variation in metals concentrations in the slag over time associated with differences in process feed material.[9] However, this result suggests that the

primary sampling site, site A, was representative of other locations in eastern Iowa with slag-covered rural roads. The comparison between site A and site B was limited by the small number of dichotomous sampler filters (8) analyzed for PM and PM metals for site B.

Distribution of metals in the road dust compared to the airborne PM

Correlations between proportions of metals in the road dust and metals in the airborne dust (PM_{10}) were calculated (Table S11†). The correlations were limited to the metals analyzed by all three methods (ACMM, ICP-MS PM, and ICP-MS road dust): Al, Cr, Mn, Fe, Co, Ni, Cu, As, Pb, V, Zn, and excluded metals with results less than the detection limit (Cd and Sb). Due to the difference in dust particle sizes between the road dust and the air samples, average concentrations of each metal analyzed by all three methods were compared to the total concentrations of these metals to determine whether the proportions of each metal were consistent between the three methodologies. There was a significant correlation between metals proportions by ICP-MS analysis when comparing PM_{10} samples to the road dust samples ($p = 0.007$), and significant correlations ($\alpha < 0.001$) were also observed when comparing the ACMM results to the road dust ICP-MS results and to the PM_{10} ICP-MS results, that is, the proportions of metals in the road dust were similar to the proportions of metals in the PM_{10}.

Analysis of factors potentially affecting manganese concentrations

Multiple linear regression analysis to obtain potential factors affecting manganese concentrations was conducted. The analysis was limited to data representing times when the wind was blowing from the roadway toward the monitoring devices. The model was run with three different values for wind direction (Table 3). These three values represent the cosine of the angle resulting from the adjustment of wind direction to road angle, which was necessary because the road, while straight in the study area, is orientated approximately from the west-northwest to the east-southeast. After this adjustment, wind blowing parallel to the road would be represented by a cosine of 0. The overall model adjusted R-squared was 0.65 and the overall model p-value was < 0.001. The wind speed was significant at $\alpha = 0.05$, while the wind direction and the interaction of traffic count and wind direction were significant at $\alpha = 0.001$ and $\alpha = 0.01$, respectively (Table 4). However, wind direction was not individually considered a determinant of manganese

Table 3 Values in the model representing wind direction in relation to the road

Value	Wind direction
0.2	Near parallel to the road, blowing from the road to the monitors
0.5	An intermediate value, blowing from the road to the monitors
1.0	Perpendicular to the road, blowing from the road to the monitors

Table 4 Results of the statistical run ($n = 185$), summarizing residuals, coefficients, and levels of significance

Coefficients:	Estimate	Std. error	Pr(>|t|)
(Intercept)	6.84	0.82	< 0.001
Wind speed	0.105	0.053	0.050
RH	0.0167	0.0086	0.055
Traffic count	−0.0452	0.084	0.59
Wind direction	−3.43	0.83	< 0.001
Traffic: wind dir.	0.300	0.095	0.002

concentration because its significant interaction with traffic count violates the assumption of heterogeneity of regression slopes.

Manganese concentrations are more sensitive to traffic count as the wind shifts from parallel to perpendicular to the road (Fig. 2), illustrating the significant interaction between traffic counts and wind direction. The highest modeled concentrations for the perpendicular wind are lower than the concentrations for the smaller angles, presumably because the particulate plume from a passing vehicle clears the area faster, while the plume from a shallower angle would take longer to clear the area around the monitors. The plume from a car continues to be contributed to the PM sample at a fixed location by a car long after the car leaves the site (assuming "parallel" means parallel and opposite the direction of travel). Therefore, additional cars add to a built-up plume that does not diminish or increase appreciably with changes in traffic count. However, the plume concentrations during perpendicular winds increase and decrease quickly because of the cross wind, so that it takes more and more cars to create higher concentrations. The model also indicated that a one-unit increase in wind speed would result in a 10% decrease in the log of the manganese concentration, that is, changing the wind speed in the model would incrementally shift the plot up or down.

The data from this study reinforces that of Tian who found that particulate concentrations decrease as wind velocity increases,[41] but the additional strength of this research is that it simultaneously evaluated the effects of wind direction and level
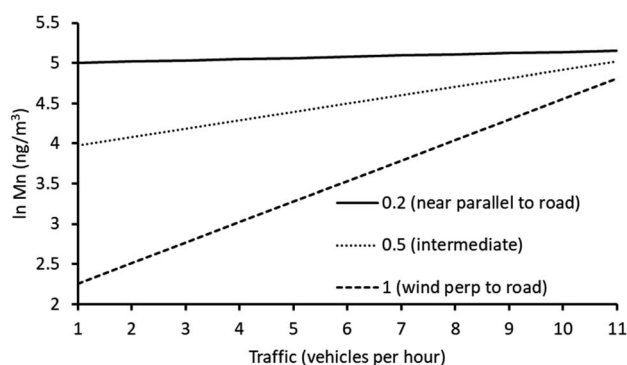

Fig. 2 Interaction plot for manganese at site A with varying wind directions relative to the road direction (perpendicular [perp], parallel, and intermediate between parallel and perpendicular) and varying traffic levels.

© 2023 The Author(s). Published by the Royal Society of Chemistry

Environ. Sci.: Atmos., 2023, **3**, 238–246 | **243**

of vehicular traffic. According to the general linear model resulting from an analysis of manganese concentrations, a wind direction parallel to the road allowed more of the dust plume to pass the instrument intakes (as the dust from upwind would follow the road) than when the wind was blowing perpendicular to the road, where only a small portion of the plume would pass the intakes and would disappear in a short time. Additionally, the closer the wind direction was to being parallel to the road, the less of an effect of traffic levels was observed, presumably because the dust plume would not clear the area around the monitor intakes as quickly as when the wind is perpendicular to the road, resulting in an effect that would approximate the concentrations observed with higher traffic levels. Since the BAM integrates the concentration over an hour, the results cannot indicate whether the ambient PM was at a low concentration for a long period or a high concentration for a short period.

This analysis was limited by lack of data on traffic speed and vehicle size. In addition, hourly PM and metal analyses were only conducted at one sample location.

Conclusions

When normalized by traffic counts, roadside particulate matter (PM_{10} and $PM_{2.5}$) concentrations did not significantly differ between a road to which EAF slag had been applied and a road to which the slag had not been applied. However, the proportion of manganese in the PM was found to be 1.30 times higher in the coarse fraction ($PM_{2.5}$–PM_{10}) of fugitive dust from roads to which the slag had been applied as compared to samples collected near roads to which the slag had not been applied, although this difference was not statistically significant. These results suggest that the addition of slag to rural gravel roads does not influence the PM concentration from dust emitted from these roads but may elevate the proportion of manganese in the PM. The lack of effect of application of the slag on PM concentrations may partially be a result of the lower level of fines in the EAF slag (around 6%) as compared to the crushed limestone (generally near 16% fines), that is, there was enough slag dust to affect the metals proportions in the PM, but not enough to noticeably increase the PM level.

Hourly measurements of Mn in the PM using the ACMM were highly correlated with hourly measurements of the total PM. However, daily Mn air sample results from the ACMM were consistently lower than and significantly different from the ICP-MS results from the filter samples. Likewise, results of ICP-MS analyses of metals in the dust collected from the road surface correlated well with ICP-MS results of filter samples, suggesting that analysis of road dust samples will aid in estimating the potential for detecting slag-related metals in the airborne dust.

When several potential factors affecting the manganese content in the airborne particulates emanating from slag-applied roads were evaluated in a statistical model, wind speed and the interaction of traffic and wind direction were found to be statistically significant. This result is important because of the effects this interaction could have on particulate and metal exposures to nearby humans. Not considering the effects of wind speed and the interaction of traffic volume and

wind direction could underestimate the human exposures and the estimate of human health risk. No previous studies were identified that described this interaction as presented here; future studies of particulate emission from unpaved roads should consider and further evaluate this interaction.

Additional studies of the use of EAF slag should be conducted to address variables beyond the scope of this study that could affect concentrations of manganese and other HAP metals in the PM_{10}, such as slag application rate, variability of the concentrations of HAP metals in the slag, and vehicle size and speed. Companion papers on this exposure scenario will address PM emissions and concentration dispersion as well as inhalation and ingestion risk from PM and manganese and other metal exposures to residents near slag-covered rural roads.

Author contributions

J. K.: conceptualization, methodology, investigation, formal analysis, data curation, writing – original draft; P. T. O.: conceptualization, methodology, project administration, funding acquisition, resources, software, supervision, writing – review & editing; R. A.: formal analysis, investigation, writing – review & editing; D. L.: formal analysis, data curation, writing – review & editing; D. M. C.: conceptualization, funding acquisition, project administration, resources, writing – review & editing.

Conflicts of interest

There are no conflicts to declare.

Acknowledgements

References

1 S. Martin and W. Griswold, *Environmental Science and Technology Briefs for Citizens, Human Health Effects of Heavy Metals*, K.S.U. Center for Hazardous Substance Research, 2009.

2 M. Kampa and E. Castanas, Human health effects of air pollution, *Environ. Pollut.*, 2008, **151**(2), 362–367.

3 EPA, *Initial List of Hazardous Air Pollutants with Modifications*, 2016, cited 2019 October 23, 2019, Available from: **https://www.epa.gov/haps/initial-list-hazardous-air-pollutants-modifications**.

4 I. Arribas, A. Santamaría, E. Ruiz, V. Ortega-López and J. M. Manso, Electric arc furnace slag and its use in hydraulic concrete, *Constr. Build. Mater.*, 2015, **90**, 68–79.

5 American Iron and Steel Institute. Steel Production, 2020, cited 2022 February 22, Available from: https://www.steel.org/steel-technology/steel-production/.

6 National_Slag_Association, *Product Applications and Types*, 2013, cited 2020 April 9, Available from: https://nationalslag.org/product-applications-and-types/.

7 H. Yi, G. Xu, H. Cheng, J. Wang, Y. Wan and H. Chen, An Overview of Utilization of Steel Slag, *Procedia Environ. Sci.*, 2012, **16**, 791–801.

8 USGS, *Iron and Steel Slag Statistics and Information*, 2021, cited 2021 August 22, Available from: https://www.usgs.gov/centers/nmic/iron-and-steel-slag-statistics-and-information?qt-science_support_page_related_con=0#qt-science_support_page_related_con.

9 C. Shi, Steel Slag—Its Production, Processing, Characteristics, and Cementitious Properties, *J. Mater. Civ. Eng.*, 2004, **16**(3), 230–236.

10 A. Moon, *Electric Arc Furnace Steel Slag, I.D.o.N. Resources*, Iowa Department of Natural Resources: Memo to County Road Officials and Iowa Department of Transportation Officials, 2006.

11 M. H. Aziz, M. R. Hainin, H. Yaacob, Z. Ali, F. L. Chang and A. M. Adnan, Characterisation and utilisation of steel slag for the construction of roads and highways, *Mater. Res. Innovations*, 2014, **18**(6), 255–259.

12 USDOT, *Gravel Roads Construction & Maintenance Guide*, F. H. A. United States Department of Transportation, 2015.

13 USDOT, Operational Safety of Gravel Roads, in *Rural and Tribal Communities: Vulnerability to Structural Failures and GeoHazards, U.T.U.T.C. Center for Safety Equity in Transportation*, CSET, University of Alaska Fairbanks, 2019, p. 40.

14 J. Creuzer, C. L. M. Hargiss, J. E. Norland, *et al.*, Does Increased Road Dust Due to Energy Development Impact Wetlands in the Bakken Region?, *Water, Air, Soil Pollut.*, 2016, **227**, 39, 14.

15 G. Tian, S. B. Fan, Y. H. Huang, L. Nie and G. Li, Relationship between wind velocity and PM10 concentration & emission flux of fugitive dust source, *Huanjing Kexue*, 2008, **29**(10), 2983–2986.

16 S. Tian, T. Liang and K. Li, Fine road dust contamination in a mining area presents a likely air pollution hotspot and threat to human health, *Environ. Int.*, 2019, **128**, 201–209.

17 D. Knight, N. A. Ramos, C. R. Iceman and S. M. Hayes, Is Unpaved Road Dust Near Fairbanks, Alaska a Health Concern? Examination of the Total and Bioaccessible Metal(loid)s, *J. Young Investig.*, 2017, **33**(1), 8–18.

18 R. Khan and M. A. Strand, Road Dust and its Effect on Human Health: a Literature Review, *Epidemiol. Health*, 2018, e2018013, 11.

19 C. Claiborn, A. Mitra, G. Adams, L. Bamesberger, G. Allwine and R. Kantam, Evaluation of PM10 Emission Rates from Paved and Unpaved Roads Using Tracer Techniques, *Atmos. Environ.*, 1995, **29**(10), 1079–1085.

20 D. Williams, M. Shukla and J. Ross, Particulate Matter Emission by a Vehicle Running on Unpaved Road, *Atmos. Environ.*, 2008, **42**, 3899–3905.

21 Y. Du, B. Gao, H. Zhou, X. Ju, H. Hao and S. Yin, Health Risk Assessment of Heavy Metals in Road Dusts in Urban Parks of Beijing, China, *Procedia Environ. Sci.*, 2013, **18**, 299–309.

22 H. Chen, B. Wang, D. S. Xia, Y. J. Fan, H. Liu, Z. R. Tang and S. Ma, The influence of roadside trees on the diffusion of road traffic pollutants and their magnetic characteristics in a typical semi-arid urban area of Northwest China, *Environ. Pollut.*, 2019, **252**, 1170–1179.

23 S. Chen, X. Zhang, J. Lin, J. Huang, D. Zhao, T. Yuan, K. Huang, Y. Luo, Z. Jia, Z. Zang, Y. Qiu and L. Xie, Fugitive Road Dust $PM_{2.5}$ Emissions and Their Potential Health Impacts, *Environ. Sci. Technol.*, 2019, **53**(14), 8455–8465.

24 T. Gonet and B. A. Maher, Airborne, Vehicle-Derived Fe-Bearing Nanoparticles in the Urban Environment: A Review, *Environ. Sci. Technol.*, 2019, **53**(17), 9970–9991.

25 W. Maeaba, S. Prasad and S. Chandra, First Assessment of Metals Contamination in Road Dust and Roadside Soil of Suva City, Fiji, *Arch. Environ. Contam. Toxicol.*, 2019, **77**(2), 249–262.

26 S. Xu, N. Zheng, J. Liu, Y. Wang and S. Chang, Geochemistry and health risk assessment of arsenic exposure to street dust in the zinc smelting district, Northeast China, *Environ. Geochem. Health*, 2013, **35**(1), 89–99.

27 M. Yamaya, K. Zayasu, T. Fukushima, K. Sekizawa, S. Shimura, H. Sasaki and T. Takishima, Inhalation of road dust by residents in polluted areas, *Arch. Environ. Health*, 1992, **47**(2), 131–134.

28 D. Shi and X. Lu, Contamination Levels and Source Analysis of Heavy Metals in the Finer Particles of Urban Road Dust from Xi'an, China, *Huanjing Kexue*, 2018, **39**(7), 3126–3133.

29 G. Sun, Z. Li, T. Liu, J. Chen, T. Wu and X. Feng, Metal Exposure and Associated Health Risk to Human Beings by Street Dust in a Heavily Industrialized City of Hunan Province, Central China, *Int. J. Environ. Res. Public Health*, 2017, **14**(3), 261–271.

30 N. Soltani, B. Keshavarzi, F. Moore, T. Tavakol, A. R. Lahijanzadeh, N. Jaafarzadeh and M. Kermani, Ecological and Human Health Hazards of Heavy Metals and Polycyclic Aromatic Hydrocarbons (PAHs) in Road Dust of Isfahan Metropolis, Iran, *Sci. Total Environ.*, 2015, 712–723.

31 H. Lee, H. T. Chon, M. Sager and L. Marton, Platinum pollution in road dusts, roadside soils, and tree barks in Seoul, Korea, *Environ. Geochem. Health*, 2012, **34**, 5–12.

32 E. Liu, T. Yan, G. Birch and Y. Zhu, Pollution and Health Risk of Potentially Toxic Metals in Urban Road Dust in Nanjing, a Mega-City of China, *Sci. Total Environ.*, 2014, 476–477.

33 S. Potgieter-Vermaak, G. Rotondo, V. Novakovic, S. Rollins and R. Van Grieken, Component-specific toxic concerns of the inhalable fraction of urban road dust, *Environ. Geochem. Health*, 2012, **34**(6), 689–696.

34 S. Kong, B. Lu, Y. Ji, X. Zhao, Z. Bai, Y. Xu, Y. Liu and H. Jiang, Risk assessment of heavy metals in road and soil

© 2023 The Author(s). Published by the Royal Society of Chemistry

Environ. Sci.: Atmos., 2023, **3**, 238–246 | **245**

dusts within PM2.5, PM10 and PM100 fractions in Dongying city, Shandong Province, China, *J. Environ. Monit.*, 2012, **14**(3), 791–803.

35 S. Kaur and M. J. Nieuwenhuijsen, Determinants of Personal Exposure to PM2.5, Ultrafine Particle Counts, and CO in a Transport Microenvironment, *Environ. Sci. Technol.*, 2009, **43**(13), 4737–4743.

36 USGS, *Manganese—It Turns Iron into Steel (and Does So Much More)*, USGS Mineral Resources Program, U.S.G. Survey, 2014, p. 2.

37 S. Schmitz, Re: Toxicity of EAF Slag on Roads in Muscatine, Iowa, in December 28, 2018 Email to Edward Askew, 2018, 3.

38 IDPH, *Health Consultation – Steel Slag on County Roads, Muscatine County*, Iowa, I. D. o. P. Health, 2020, p. 114.

39 D. Eller, Steel slag used on rural Iowa roads could be harming children, report shows, in *Des Moines Register*, 2019.

40 EPA, *Compendium Method IO-2.2, Sampling of Ambient Air for PM10 using an Andersen Dichotomous Sampler*, Center for Environmental Research Information, Office of Research and Development, U.S.E.P. Agency, Cincinnati, OH, 1999.

41 IDOT, *Aggregate Gradation Table*, I.D.o.Transportation, 2009.

42 K. White, *Questions about Slag Specifications*, ed. J. Kacer, 2022.

43 M. Maslehuddin, A. M. Sharif, M. Shameem, M. Ibrahim and M. S. Barry, Comparison of properties of steel slag and crushed limestone aggregate concretes, *Constr. Build. Mater.*, 2003, **17**(2), 105–112.

44 EPA, *Method 6010b, Inductively Coupled Plasma-Atomic Emission Spectrometry*, U.S.E.P. Agency, 1996.

45 EPA, *Method 6020, Inductively Coupled Plasma - Mass Spectrometry*, U.S.E.P. Agency, 1994.

46 EPA, *Method 7471a, Mercury in Solid or Semisolid Waste Manual Cold-Vapor Technique*, U.S.E.P. Agency, 1994.

47 L. Lutterotti, S. Matthies and H. Wenk, *MAUD: A Friendly Java Program for Material Analysis using Diffraction*, IUCr: Newsletter of the Commission on Powder Diffraction, 1999, vol. 21, pp. 14–15.

48 F. Engström, *et al.*, Leaching Behavior of Aged Steel Slags, *Steel Res. Int.*, 2014, **85**(4), 607–615.

49 EPA, *List of Designated Reference and Equivalent Methods*, United States Environmental Protection Agency, Research Triangle Park, NC, issue date June 15, 2020.

50 W. Hinds, *Aerosol Technology: Properties, Behavior, and Measurement of Airborne Particles*, Wiley-Interscience, Singapore, 2nd edn, 1999, vol. 1, p. 483.

51 Beacon, *Muscatine Area Geographic Information Consortium (MAGIC)*, 2020, November 28, 2020, Available from: **https://beacon.schneidercorp.com/Application.aspx?AppID=12&LayerID=93&PageTypeID=1&PageID=950&KeyValue=0507300018**.

52 R Core Team. R, *A Language and Environment for Statistical Computing*, 2020, Available from: **https://www.R-project.org/**.

53 EPA, *NAAQS Table*, 2021 February 10, cited 2021 August 30, Available from: **https://www.epa.gov/criteria-air-pollutants/naaqs-table**.